MSU RE-ACCELERATOR – THE RE-ACCELERATION OF LOW ENERGY RIBS AT THE NSCL*

X. Wu[#], G. Bollen, M. Doleans, T. L. Grimm[†], W. Hartung, F. Marti, S. Schwarz,
R. C. York and Q. Zhao

National Superconducting Cyclotron Laboratory, Michigan State University, E. Lansing,
MI 48824, USA

Abstract

The in-flight Particle Fragmentation (PF) method for producing Rare Isotope Beams (RIBs) has been used at the National Superconducting Cyclotron Laboratory (NSCL) at Michigan State University (MSU) since 1989. The upgraded Coupled Cyclotron Facility (CCF) has been in operation for nuclear physics research since 2001 with the experimental program largely utilizing PF produced RIBs. To provide new research opportunities for an experimental program ranging from low-energy coulomb excitation to transfer reaction studies of astrophysical reactions, a novel system is proposed at the NSCL to first stop the high energy RIBs in a helium filled gas system, then increase their charge state with an Electron Beam Ion Trap (EBIT) charge breeder, and finally re-accelerate them to about 3 MeV/u using a radio frequency quadrupole (RFQ) followed by a superconducting linac. The superconducting linac will use quarter-wave resonators with optimum β (β_{opt} = β value for which the cavity delivers the maximum accelerating voltage) of 0.041 and 0.085 for acceleration, and superconducting solenoid magnets for transverse focusing. An upgrade option to achieve a beam energy up to ~12 MeV/u with additional accelerating cryomodules is also possible. This paper will discuss the accelerator system design and beam dynamics simulations for the MSU Re-accelerator project.

INTRODUCTION

Isotope Separation On-line (ISOL) and Projectile Fragmentation (PF) are the two methods to produce high quality RIBs for the nuclear science community. With ISOL, RIBs are first produced at rest by high-energy stable beams from the production accelerator hitting a thick and hot target. They are then extracted through to an ion source followed by an isotope/isobar separator and eventually re-accelerated by a post accelerator to the desired energy. RIBs produced by the ISOL method have high beam quality and low beam energy, but are limited to isotopes with longer lifetimes (τ >1s). Isotope extraction and ionization efficiency depend on the element's chemical properties and the most neutron-rich isotopes will have intensities that are too low and lifetimes that are too short to be suitable for re-acceleration. With the PF method, RIBs are produced at velocity by high-energy stable beams from the production accelerator hitting a thin production target and separated in-flight by a magnetic fragmentation separator. The RIBs produced by PF have a more modest beam quality and a higher beam energy (E/A >50 MeV/u) than those produced by the ISOL method, but very short-lived isotopes (τ >10^{-6}s) are possible. With the physical method of separation, no chemistry is involved in the RIBs production. However, the creation of low-energy RIBs by PF is difficult and the beam emittance becomes large.

Since 1989, the NSCL has been using the PF method with great success to produce fast RIBs for nuclear structure and nuclear reaction experiments. Figure 1 shows the conceptual view of the existing fast RIB facility and planned low energy RIB facility at the NSCL. The high energy primary beams are produced by two coupled superconducting cyclotrons, and the RIBs are separated in-flight by the A1900 Fragment Separator. To provide new research opportunities with low-energy RIBs, the NSCL is developing a prototypical facility to demonstrate the technical feasibility and performance characteristics for stopping and re-accelerating RIBs produced and separated in-flight. This is an important step towards a next-generation rare isotope facility in the United States.
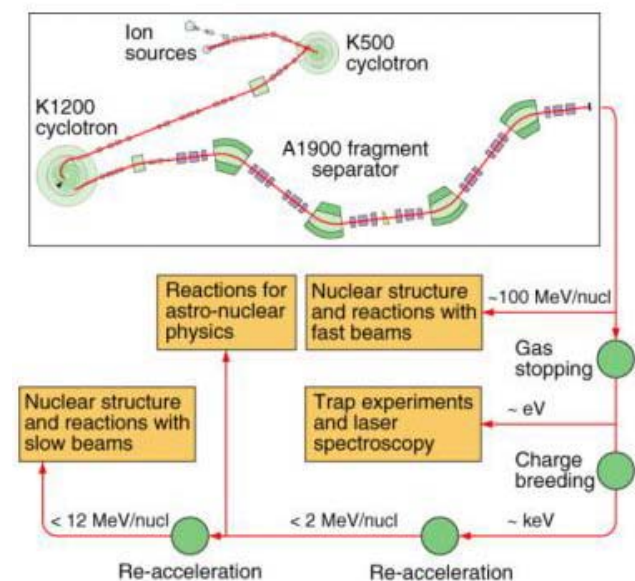
Figure 1: A conceptual view of the planned facility for stopping and re-accelerating RIBs produced and separated in-flight at the NSCL.

The low-energy RIB facility at the NSCL will require three key steps: gas stopping of the PF-produced RIBs in a gas cell; breeding the stopped RIBs to high charges in a EBIT charge breeder; and re-accelerating the RIBs in a superconducting linac.

GAS STOPPING AND EBIT CHARGE BREEDER

Gas cells have been used to slow down and stop fast RIBs. A gas cell system at the NCSL was the first to demonstrate stopping of fast (~100MeV/u) RIBs [1]. The linear gas cell uses a combination of solid degraders and a helium-gas-filled chamber at a pressure of up to 1 bar to slow down and stop the fast RIBs. Static electric fields inside the chamber are used to guide the RIBs to the extraction nozzle and the gas flow extracts the low-emittance, low-energy RIBs from the gas cell.

The linear gas cells have shown intensity-dependent extraction efficiencies and long extraction times (~100 ms) which will result in decay loss of short-lived RIBs, losing the advantage of PF and in-flight separation methods. In addition, the stopping efficiencies for light RIBs are significantly lower. The NSCL is evaluating alternative configurations with a longer stopping path and lower helium gas pressure that could provide shorter extraction times and higher beam rate capability [2].

The low-energy RIB facility at the NSCL will allow the possibility of both a linear gas cell, or an alternative geometry referred to as a cyclotron gas stopper to slow down and stop the fast RIBs produced and separated in-flight. Figure 2 shows the layout of the planned NSCL gas stopping system with the possibility of using either gas stopping method.
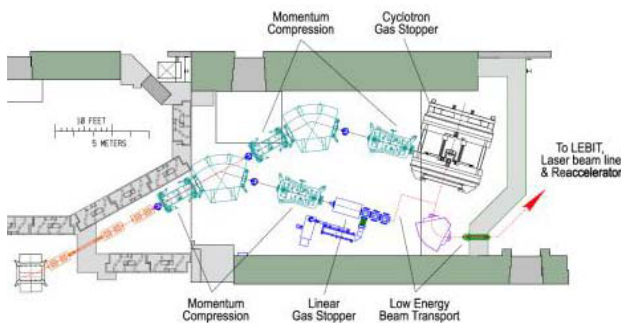
Figure 2: The layout of the planned NSCL gas stopping system.

After the mass separator, the low-energy (~kV) and singly-charged RIBs are extracted from the gas stopper. To achieve more compact and cost-effective reacceleration of the stopped RIBs, an EBIT will be used to boost the charge state of the RIBs to a charge-to-mass ratio of about 0.25. The charge-breeding scheme was first demonstrated with REX-ISOLDE at CERN [3]. Since the EBIT charge breeder recently developed for the TITAN project at TRIUMF [4] has the expected performance close to that required for the low-energy RIB facility at

the NSCL, its design has been chosen as the basis for the NSCL EBIT charge breeder, as shown in Figure 3 [5]. The EBIT will be located on a ~60 kV high voltage platform to match the velocity of the RIBs to that appropriate for injection into the radio frequency quadrupole (RFQ) of the re-accelerator.
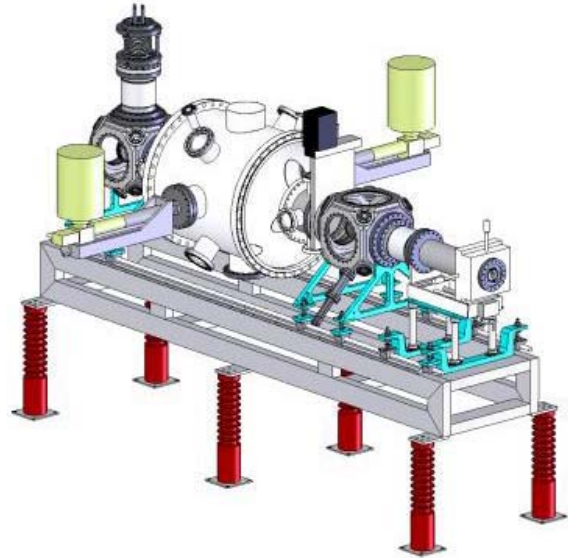
Figure 3: EBIT charge breeder for the low-energy RIB facility at the NSCL.

RE-ACCELERATOR

The re-accelerator is required to accelerate RIBs from the EBIT with charge-to-mass ratio (Q/A) ranging from 0.2 to 0.4 and to achieve a final energy from 0.3 to 3 MeV/u. In addition, an upgrade path to an output energy of 12 MeV/u is incorporated. The requirements for the bunch width and energy spread for the RIBs on target are 1 ns and 1 keV/u, corresponding to a longitudinal emittance of ~0.25 π keV/u-ns. The beam spot on target is required to be ~1 mm. The EBIT will have a variable extraction voltage to achieve a fixed RFQ input energy of 12 keV/u for ions with charge-to-mass ratios varying from 0.2 to 0.4. From simulations, the longitudinal emittance after the RFQ is mainly determined by the initial energy spread of the beam from the EBIT. For the end-to-end beam simulations, the normalized transverse beam emittance from the EBIT was assumed to be 0.6π mm-mrad with a maximum energy spread of $\pm$ 0.2%, based on experience with an operating EBIS at REX-ISOLDE.

The proposed accelerator system consists of four segments: a Low Energy Beam Transport (LEBT) system to transport, bunch and match the RIBs from the EBIT to the RFQ, an RFQ for initial beam acceleration and focusing, a superconducting linac system for RIBs acceleration to the desired energy, and a High Energy Beam Transport (HEBT) system to deliver the RIBs to an experimental area with the required beam parameters. The entire accelerator system and the beginning of the experimental area will be located on a balcony in the

NSCL high bay area. Figure 4 shows the layout of the proposed accelerator system [6].
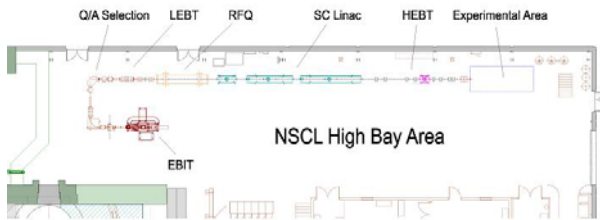
Figure 4: The layout of the proposed re-accelerator to the beginning of experimental area.

The re-accelerator design benefits significantly from the past Rare Isotope Accelerator (RIA) driver linac R&D efforts at the NSCL. For example, the front-end design was derived from that of the RIA driver linac. Also, the superconducting linac uses the same 80.5 MHz $\lambda/4$ cavities as the RIA driver linac. Both structures with β_{opt} of 0.041 and 0.085 have already been prototyped in 2003 and 2007; both exceeded the design requirements [7,8]. In addition, the design and construction of the re-accelerator will provide valuable experience for future projects such as the proposed Isotope Science Facility (ISF) at MSU [9].

End-to-end beam simulations of the re-accelerator using various computer codes were performed to evaluate the performance of the proposed accelerator system and determine the hardware specifications. Beam simulations through the LEBT and RFQ were investigated using RIAPMTQ [10]. IMPACT [10] and a linear beam dynamics code developed at the NSCL were used for beam simulation studies in the superconducting linac section and HEBT. DIMAD and TRACE3D were used to study transverse focusing, beam matching, and the effect of misalignment and a correction scheme in the superconducting linac section.

Low Energy Beam Transport (LEBT)

The LEBT uses four electrostatic quadrupoles and two solenoid magnets to provide transverse focusing for the RIBs from the EBIT charge breeder after *Q/A* selection. To achieve a small longitudinal emittance, an external Multi-Harmonic Buncher (MHB) is used prior to the RFQ. The location and the voltages of the different harmonics of the MHB were optimized to match the beam longitudinally into the RFQ and achieve a high capture efficiency of ~82%.

The end-to-end beam simulations begin with the RIBs after *Q/A* selection with an energy of 12 keV/u and a *Q/A* of 0.25. The simulations assume a normalized transverse emittance of 0.6π mm-mrad and an energy spread of $\pm 0.2\%$, as mentioned above. Figure 5 shows the initial phase space of the RIBs at the entrance of the LEBT.
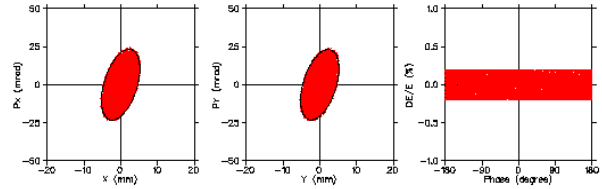
Figure 5: Horizontal (left), vertical (middle), and longitudinal (right) phase space at the entrance of the LEBT. The black ellipses represent the 90% emittance.

The beam through the LEBT was simulated using RIAPMTQ. The phase space at the entrance of the RFQ is shown in Figure 6. The beam is bunched and matched into the RFQ at this location. No transverse emittance growth in the LEBT is predicted.
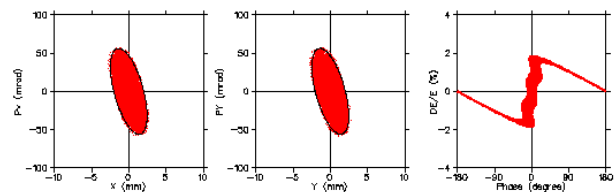
Figure 6: Horizontal (left), vertical (middle), and longitudinal (right) phase space at the entrance to the RFQ.

Radio Frequency Quadrupole (RFQ)

Benefiting from the higher *Q/A* ratio of the RIBs from the EBIT, the re-accelerator RFQ [11] can achieve an output energy of 600 keV/u. This energy is higher than the 300 keV/u design values of the RIA driver linac and improves the beam dynamics performance of the superconducting linac due to the increase in longitudinal acceptance.

Since the RIBs are already bunched at the entrance of RFQ by the upstream multi-harmonic buncher, the RFQ can achieve a higher acceleration efficiency while maintaining a smaller longitudinal emittance of the core beam with an initial synchronous phase of -20° and a modulation factor of 1.15. These values are a compromise to achieve a reasonable ratio between the longitudinal acceptance and emittance. At the entrance to the RFQ, a 4-cell radial matching section was used, followed by an entrance transition cell. At the exit of the RFQ, a transition cell will bring the vanes to quadrupole symmetry, followed by an exit fringe-field region to obtain an output beam with similar Twiss parameters in both the horizontal and vertical planes to match to the downstream solenoid focusing. A constant inter-vane voltage of ~85 kV was adopted in the design, resulting in a vane length of 3.33 m. Figure 7 shows the initial longitudinal distribution of a *Q/A* = 0.2 beam at the RFQ entrance, together with the RFQ longitudinal acceptance. Table 1 lists the main design parameters of the CW RFQ for the re-accelerator.
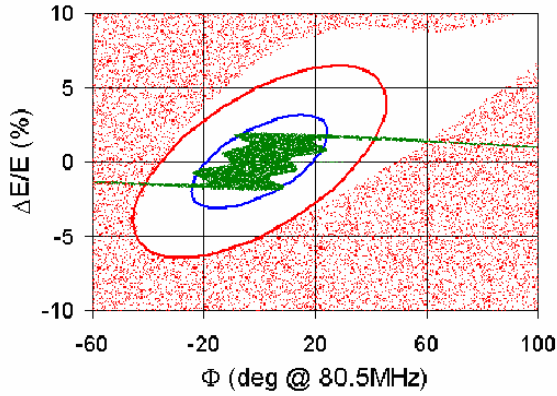
Figure 7: The longitudinal acceptance (white area) of the RFQ and its maximum fitted ellipse (red line). The longitudinal distribution of a $Q/A = 0.2$ beam (green dots) at the entrance of the RFQ and a minimum ellipse (blue line) fitted for the core particles are also shown.

Table 1: Main RFQ design parameters.

Frequency (MHz)	80.5
Inter-vane voltage (kV)	86.2
Charge-to-mass ratio	0.2 – 0.4
Input energy (keV/u)	12
Output energy (keV/u)	600
Peak field ($E_{kilpatrick}$)	1.6
Peak electric field (MV/m)	16.7
Number of cells	94
Mid-cell radial aperture (mm)	7.3
Vane tip radius (mm)	6.0
Focusing strength	~4.9
Modulation factor	1.15 – 2.58
Synchronous phase (degree)	-20

The output phase space from the RFQ is shown in Figure 8. The growth of the transverse emittance in the RFQ is very small, whereas the 90% longitudinal emittance out of the RFQ is only 0.29 π keV/u-ns. The energy spread of the beam injected into the RFQ has a significant impact on the longitudinal emittance from the RFQ. To meet the requirements for bunch width and energy spread on target, a small energy spread for the beam from the EBIT is crucial. With an initial beam energy spread of ±0.2%, the 99.5% longitudinal emittance is within ~2.1 π keV/u-ns.
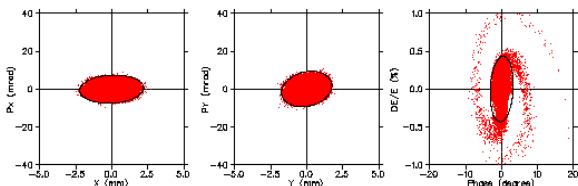
Figure 8: Horizontal (left), vertical (middle), and longitudinal (right) phase space at the exit of the RFQ.

Superconducting linac

A superconducting linac will provide the acceleration or deceleration of the RIBs from RFQ output energy of 600 keV/u to the desired final energies ranging from 0.3 to 3 MeV/u on target. A superconducting linac provides a high accelerating gradient for CW operation (100% duty factor) while requiring little rf power.

Superconducting Radio Frequency (SRF) quarter-wave ($\lambda/4$) cavities with β_{opt} of 0.041 and 0.085 are used for the superconducting linac. Table 2 shows selected RF and geometrical parameters and Figure 9 shows drawings of the $\lambda/4$ cavities. Both cavities have been prototyped and tested. Figures 10 and 11 show the Nb parts before and after welding. Figure 12a shows the $\beta_{opt} = 0.041$ prototype cavity during assembly onto the insert for RF testing. Figure 12b shows the $\beta_{opt} = 0.085$ prototype cavity just prior to insertion into the vertical cryostat.

Table 2: Selected RF and geometrical parameters for the $\lambda/4$ SRF cavities.

Cavity type	$\lambda/4$	$\lambda/4$
Optimum β	0.041	0.085
Frequency (MHz)	80.5	80.5
E_p (MV/m)	16.5	20.0
V_{acc} (MV)	0.46	1.18
E_{acc} (MV/m)	4.84	5.62
B_p (mT)	28.3 mT	46.5 mT
Temperature (K)	4.5	4.5
Length (m)	0.095	0.21
Aperture (mm)	30	30
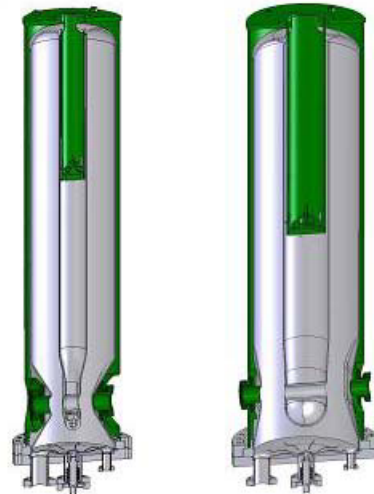
Figure 9: Superconducting accelerating structures for the re-accelerator.
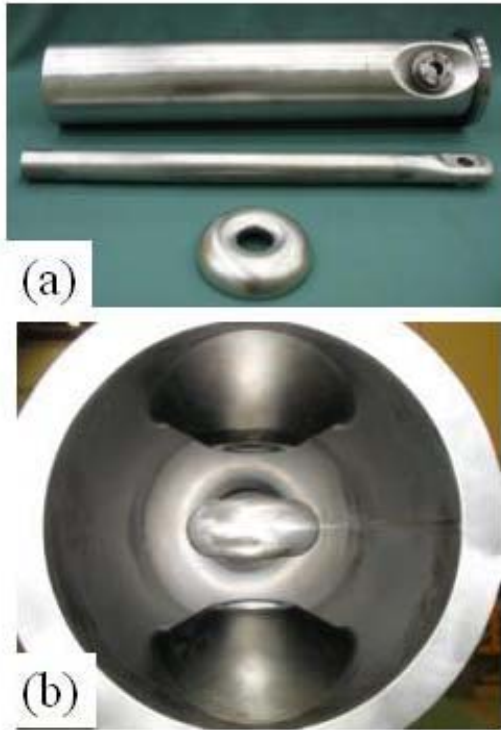
Figure 10: (a) Nb parts for the $\beta_{opt} = 0.041$ $\lambda/4$ cavity and (b) inside view of the complete cavity.
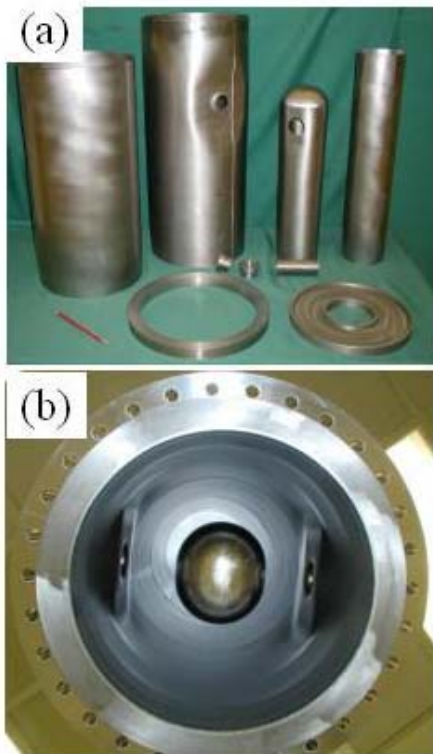
Figure 11: (a) Nb parts for the $\beta_{opt} = 0.085$ $\lambda/4$ cavity and (b) inside view of the complete cavity.

Figure 12: Photographs of (a) $\beta_{opt} = 0.041$ and (b) $\beta_{opt} = 0.085$ cavities on the RF test stand.

Figures 13 and 14 show the RF test results for both cavities, which exceed the design field levels by a comfortable margin.
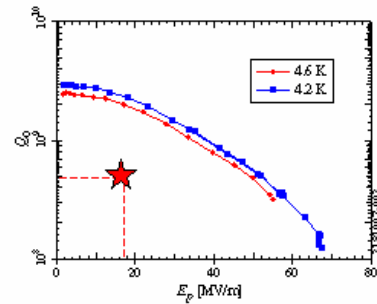
Figure 13: RF tests for the $\beta_{opt} = 0.041$ cavity at 4.2 K and 4.6 K. The design goal of 16.5 MV/m with Q_0 of 5×10^8 is also shown.
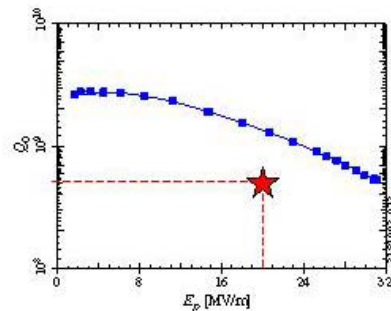
Figure 14: RF test of the $\beta_{opt} = 0.085$ cavity at 4.2 K. The design goal of 20 MV/m with Q_0 of 5×10^8 is also shown.

A total of three cryomodules, consisting of fifteen 80.5 MHz $\lambda/4$ SRF cavities, will be used in the superconducting linac section. Eight superconducting solenoid magnets inside the cryomodules, each with a peak magnetic field of 9 T, will provide transverse focusing. Each solenoid will have two dipole coils to provide alignment error corrections.

The first cryomodule will have two solenoids and one $\lambda/4$ SRF cavity with $\beta_{opt} = 0.041$ to provide transverse and longitudinal matching into the two following accelerating croyomodules. The second cryomodule will have three solenoids and six $\lambda/4$ SRF cavities with $\beta_{opt} = 0.041$ to accelerate the RIBs to ~1.2 MeV/u. Since the experimental program may require a RIB energy less than the RFQ output of 600 keV/u, this cryomodule can also be used to decelerate the RIBs to ~300 keV/u. The third cryomodule will have three solenoids and eight $\lambda/4$ SRF cavities with $\beta_{opt} = 0.085$ to accelerate the RIBs to up to ~ 3 MeV/u. For cases with final beam energy below 3 MeV/u, some SRF cavities can be used for rebunching. Figures 15 and 16 show the layout of the second and third cryomodules.
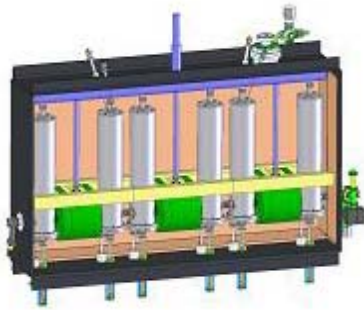
Figure 15: The layout of the second cryomodule for the re-accelerator.
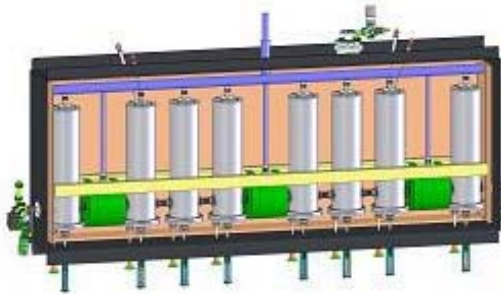
Figure16: The layout of the third cryomodule for the re-accelerator.

A prototype cryomodule [12] was designed and fabricated at the NSCL recently, as shown in Figure 17. The module consists of a 80.5 MHz $\beta_{opt} = 0.085$ $\lambda/4$ cavity and a 322 MHz $\beta_{opt} = 0.285$ $\lambda/2$ cavity, with helium vessels made of titanium. The superconducting focusing magnets inside the cryomodule consist of a 9 T solenoid with an integrated steering dipole and a 31 T/m quadrupole. Currently the RF test of the cryomodule is in progress.
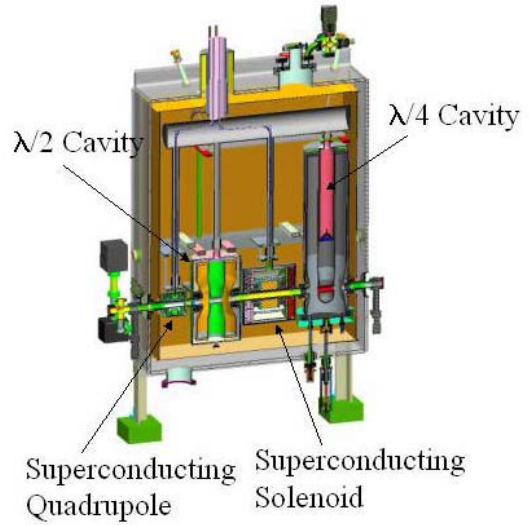
Figure 17: Prototype cryomodule with $\lambda/4$ and $\lambda/2$ cavities and focusing elements.

The beam envelope and longitudinal betatron function along the superconducting linac for the case of acceleration to ~3 MeV/u are shown in Figure 18. The linac has adequate transverse and longitudinal acceptance. No transverse emittance growth was observed. The 90% longitudinal emittance growth was only ~7%. No parametric resonance was observed in the beam simulations. Figure 19 shows the resultant phase space at the exit of the linac.
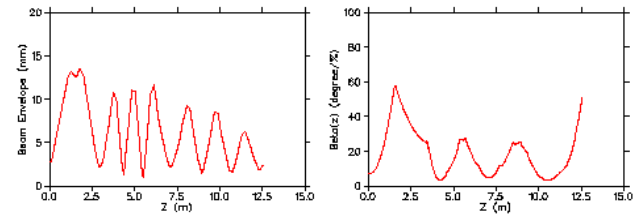
Figure 18: Beam envelope (left) and longitudinal betatron function (right) in the SC linac for RIBs accelerated to ~ 3 MeV/u.
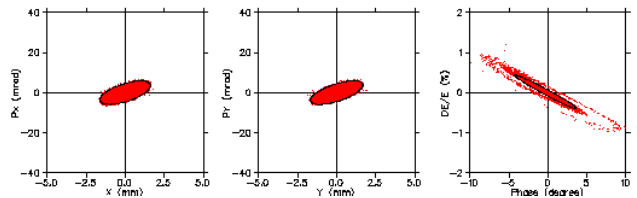
Figure 19: Horizontal (left), vertical (middle), and longitudinal (right) phase space at the exit of SC linac for RIBs accelerated to ~ 3 MeV/u.

Beam simulations for the case of RIB decelerated to ~300 keV/u were also performed with similar results. Due to the decrease in beam energy, the longitudinal phase advance is larger, but no transverse emittance growth was observed, and the 90% longitudinal emittance growth was only ~10%.

High Energy Beam Transport (HEBT)

The longitudinal phase space shown in Figure 15 has a small phase width of about ±5° (~0.3 ns) and a large energy spread of about ±1.0% with a beam energy of about 3 MeV/u. To satisfy the requirements of the bunch width and energy spread on target, the HEBT uses a π-phase advance cell consisting of four quadrupoles and a cryomodule with a single $\lambda/4$ SRF cavity with β_{opt} = 0.041. The beam bunch will first pass through the π phase advance cell and drift longitudinally with adequate transverse focusing. Then the $\lambda/4$ SRF cavity will rotate the longitudinal phase space, minimizing the beam energy spread. The last segment of the HEBT will be a final focusing cell consisting of four quadrupoles and a superconducting solenoid magnet to achieve a beam spot of ~1 mm on target. In this cell, the change in bunch length is negligible due to the small energy spread after the rebuncher cavity.

The beam envelope and longitudinal betatron function along HEBT for the case of acceleration to ~3 MeV/u are shown in Figure 20. Figure 21 shows the beam phase space and Figure 22 shows the time and energy spread distributions on the target for a beam accelerated to 3.0 MeV/u. About 88% of beam on target was within the required bunch width and energy spread of 1 ns and 1 keV/u, respectively.
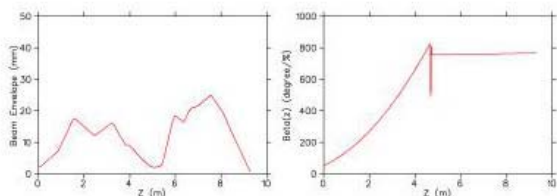
Figure 20: Beam envelope (left) and longitudinal betatron function (right) along HEBT for RIBs accelerated to ~ 3 MeV/u.
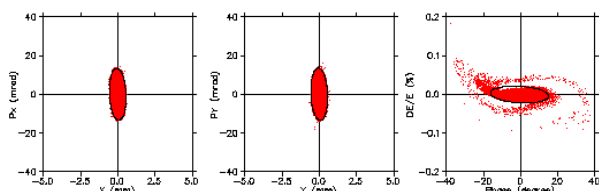
Figure 21: Horizontal (left), vertical (middle), and longitudinal (right) phase space on the target for RIBs accelerated to 3 MeV/u.
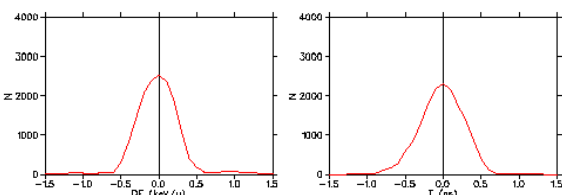
Figure 22: The time and energy spread distributions on the target for RIBs accelerated to 3 MeV/u.

Beam simulations show that the performance for the RIBs decelerated to ~300 keV/u was similar with about 89% of beam on target within the required bunch width and energy spread. Other cases within the required energy range of 300 keV/u to 3 MeV/u were simulated with similar results, demonstrating that the accelerator system design meets the performance requirements in all cases.

SUMMARY

The proposed low-energy RIB facility at the NSCL will create fast RIBs in-flight, stopping, charge breeding, and re-accelerating them efficiently and with minimum loss to provide new research opportunities for nuclear science. The baseline accelerator system for the re-accelerator has been defined and end-to-end beam simulations were performed. The results show the performance of the re-accelerator meets the anticipated requirements for the nuclear astrophysics experimental program. The RFQ construction will start in 2007. Prototype cavities for the re-accelerator have been fabricated and tested; testing of a prototype module is in progress. An upgrade for beam energies up ~12 MeV/u is possible by adding additional accelerating cryomodules.

REFERENCES

[1] S. Schwarz et al. "The Low-Energy-Beam and Ion-Trap Facility at NSCL/MSU', Nucl. Instrum. Meth. B 204 (2003) 507-511.

[2] G.K. Pang et al. "The Cyclotron Gas Stopper Project at the NSCL", Proceedings of 2007 Particle Accelerator Conference, Albuquerque, New Mexico USA, June 2007.

[3] O. Kester et al., Nucl. Instr. And Meth. B 204, 20 (2003).

[4] J. Dilling et al., Int. J. Mass. Spec. 251,198 (2006).

[5] S. Schwarz, "A high-current EBIT as a charge breeder for the re-acceleration of rare isotopes at the NSCL", to be published at ICIS 2007, Jeju, Korea.

[6] X. Wu et al. "Beam Dynamics Studies for the Reacceleration of Low Energy RIBs at the NSCL", Proceedings of 2007 PAC, Albuquerque, New Mexico USA, June 2007.

[7] W. Hartung et al. "Niobium Quarter-wave Resonator Development for the Rare Isotope Accelerator", Proceedings of the 11th Workshop on RF Superconductivity, Travemunde, Germany (2003).

[8] W. Hartung et al. "Niobium Quarter-wave Resonator Development for a Heavy Ion Re-accelerator", these proceedings.

[9] "Isotope Science Facility at Michigan State University – Upgrade of the NSCL rare isotope research capabilities", MSUCL-1345, November 2006.

[10] T. P. Wangler et al. "RIAPMTQ/IMPACT: Beam-Dynamics Simulation Tool for RIA", Proceedings of the XXIII Linac Conference, Knoxville, Tennessee USA, August 2006.

[11] Q. Zhao et al. "Design Studies of the Reaccelerator RFQ at NSCL", Proceedings of 2007 Particle Accelerator Conference, Albuquerque, New Mexico USA, June 2007.

[12] M. Johnson et al. "Cryomodule Design for a Superconducting Linac with Quarter-Wave, Half-Wave and Focusing Elements", Proceedings of 2005 Particle Accelerator Conference, Knoxville, Tennessee USA, May 2005.